Data S1.

Supplementary methods

Histopathology. Hematoxylin-eosin(HE) staining was performed routinely (hematoxylin for 2 min and eosin for 30 sec at room temperature) on a set of tissue microarrays (TMAs) (G1120; Beijing Solarbio Science & Technology Co., Ltd). On the basis of the histological features, intrahepatic cholangiocarcinoma (ICC) tissue samples were subclassified into two types: Large duct (type1) and small duct (type2).

Mucin staining using an Alcian Blue Stain Kit (pH 2.5; G1560; Beijing Solarbio Science & Technology Co., Ltd) was performed on the TMAs to distinguish the subtypes of ICC. The TMAs were stained by Alcian blue for 30 min at room temperature and scored semiquantitatively by the proportion of glandular lumens with mucin production on a scale from 0 to 2 (score 0, <10%; score 1, 10-50% and score 2, >50%) or frequent intracytoplasmic mucin.

Immunohistochemistry. The TMA sections were dewaxed and rehydrated in xylene and gradient ethanol at room temperature, respectively. After antigen retrieval, the slides were blocked with 3% hydrogen peroxide (PV-6002; Beijing Zhongshan Golden Bridge Biotechnology Co., Ltd.) for 10 min at room temperature to quench the endogenous peroxidase activity. The slides were incubated with primary antibodies (4˚C for 14h and 37˚C for 1h) and then HRP-conjugated secondary antibody (37˚C for 1 h). The sections were visualized with 3,3'-diaminobenzidine (ZLI-9017; OriGene Technologies) for 5 min at room temperature and counterstained with hematoxylin for 1 min at room temperature. Appropriate internal or external positive and negative controls were designed and used for each round, and the positive controls of S100P, BAP1, ARID1A and PBRM1antibodies were pancreatic ductal adenocarcinoma, ovarian cancer tissue, kidney and kidney tissue, respectively. The sections were observed and recorded using a light microscope (BX61, OLYMPUS).

The primary antibodies used in the present study were as follows: S100P (clone EPR6142; dilution 1:300; Abcam), BAP1 (ab199396; dilution 1:200; Abcam), ARID1A (clone EPR13501-73; dilution 1:500; Abcam) and PBRM1 (HPA015629; dilution 1:200; Sigma-Aldrich; Merck KGaA).

S100P presented nuclear and cytoplasmic staining and was evaluated semiquantitatively on the basis of the percentage of positive tumour cells: Score 0, <1%; score 1, 1-25%; score 2, 26-50%; score 3, 51-75% and score 4, 76-100%.

Analysis of IDH1/2 mutation. Genomic DNA was extracted using the QIAamp DNA FFPE Tissue Kit (56404;Qiagen GmbH) from ten 10-μm sections of ICC tissue samples-micro-dissected from formalin-fixed paraffin-embedded tissue blocks. Two pairs of primers were designed for hotspot mutations of IDH1/2. The first pair of primers for IDH1-R132 was as follows: Forward, 5'-ACACGACGCTCTTCCGATCTACACATACAAGTTGGAAATTTCTGG-3' and reverse, 5'-GACGTGTGCTCTTCCGATCTAATCACCAAATGGCACCATAC-3'. The second pair of primers for IDH2-R140 and IDH2-R172 was as follows: Forward, 5'-ACACGACGCTCTTCCGATCTCAGAGACAAGAGGATGGCTAGG-3' and reverse, 5'-GACGTGTGCTCTTCCGATCTTGTCCTCACAGAGTTCAAGCTG-3' (Tsingke Biological Technology Co., Ltd.). PCR was performed using genomic DNA, primers and GoTaq® GreenMaster Mix (M712; Promega Corporation). ThePCR thermocycling conditions used were as follows: 95˚C for 2 min, followed by 35 cycles of 94˚C for 30 sec, 60˚C for 30 sec, and 72˚C for 30 sec. Amplification products were purified using the Wizard SV Gel (concentration of 3%) and PCR Clean-up System Kit (A9281; Promega Corporation). Cycle sequencing was performed using BigDye Terminator v3.1 (Applied Biosystems; Thermo Fisher Scientific Inc.). The amplified products were separated by capillary electrophoresis on an ABI 3130xl Genetic Analyzer (Applied Biosystems; Thermo Fisher Scientific Inc.). Sequencing results were analyzed using Sequencing Analysis 5.2 and SeqScape software v,2.6 (Applied Biosystems; Thermo Fisher Scientific Inc.).

Classification of ICCs into large-duct and small-duct types. The102 cases of ICC were classified into three subtypes on the basis of histological features, S100P expression and Alcian blue staining in the first round. Among these, 8 cases (7.8%) were recognised as typical large-duct type, which met the three standards: HE, type1; S100P, score 3 or 4, and Alcian blue, score 1 or 2. In addition, 61 cases (59.8%) were typical small-duct type, which met the following conditions: HE, type2; S100P, score 0 or 1 and Alcian blue, score 0 or 1.

In the second round, the 33 cases of intermediate type were divided into two subcategories on the basis of three factors with different predictive values in the following order: HE > S100P > Alcian blue. Finally, 21 (20.6%) and 81 (79.4%) cases were identified as large-duct and small-duct-type ICC, respectively.

Figure S1. Kaplan-Meier curves showing survival rates in patients with intrahepatic cholangiocarcinoma according to PBL level. Patients with high PBL had (A) a trend toward increased disease-free survival and (B) significantly prolonged overall survival. PBL, peripheral blood lymphocyte.

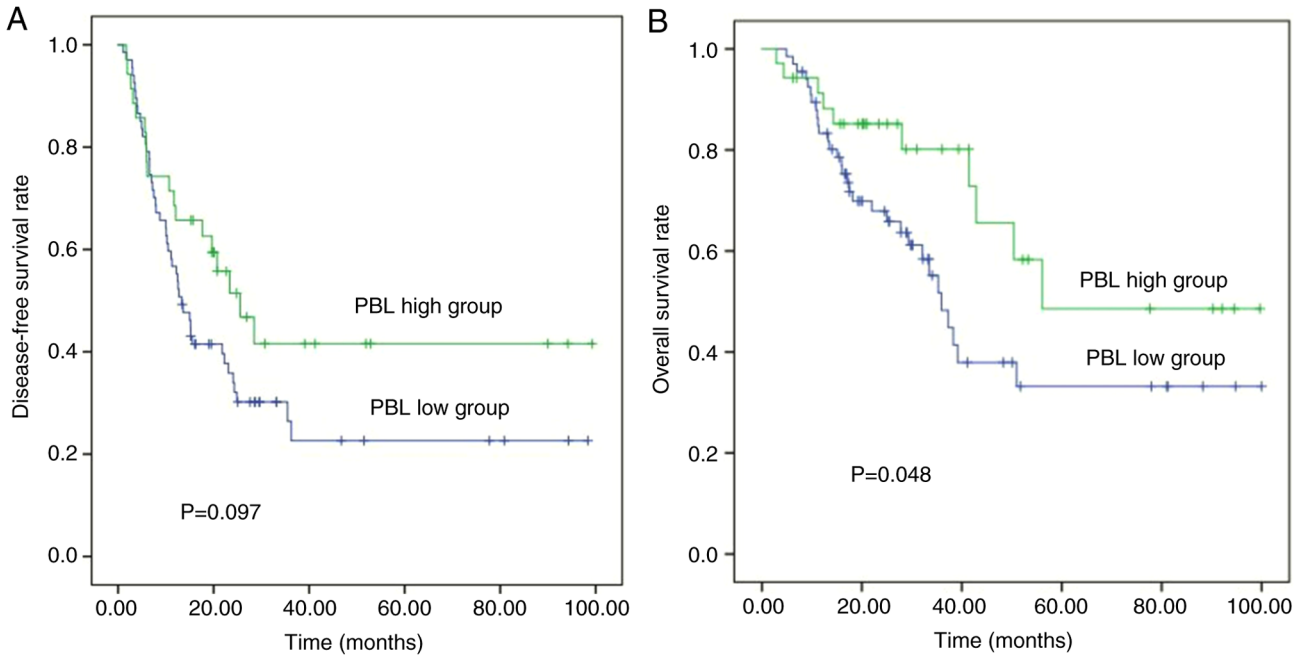

Figure S2. Kaplan-Meier curves showing $CD4^+$ TILs were not significantly associated with (A) DFS or (B)OS in patients with ICC. DFS, disease free survival; OS, overall survival; ICC, intrahepatic cholangiocarcinoma; TILs, tumor-infiltrating cells.

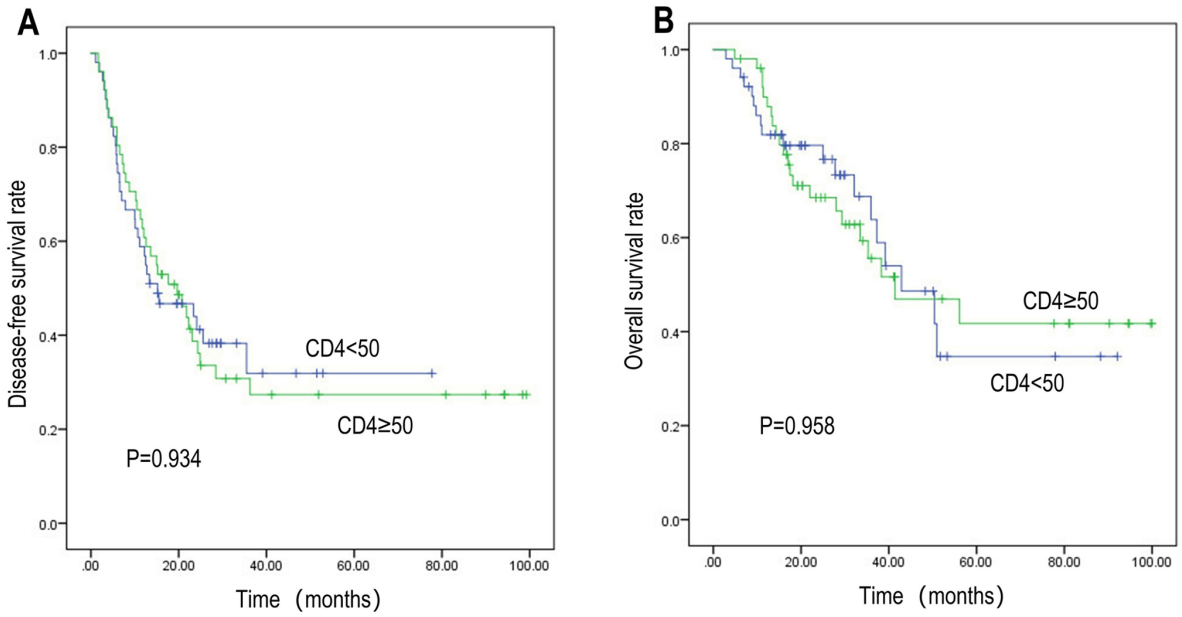

Figure S3. Kaplan-Meier curves showing $CD8^+$ TILs were not significantly associated with (A) DFS or (B) OS in patients with ICC. DFS, disease free survival; OS, overall survival; ICC, intrahepatic cholangiocarcinoma; TILs, tumor-infiltrating cells.

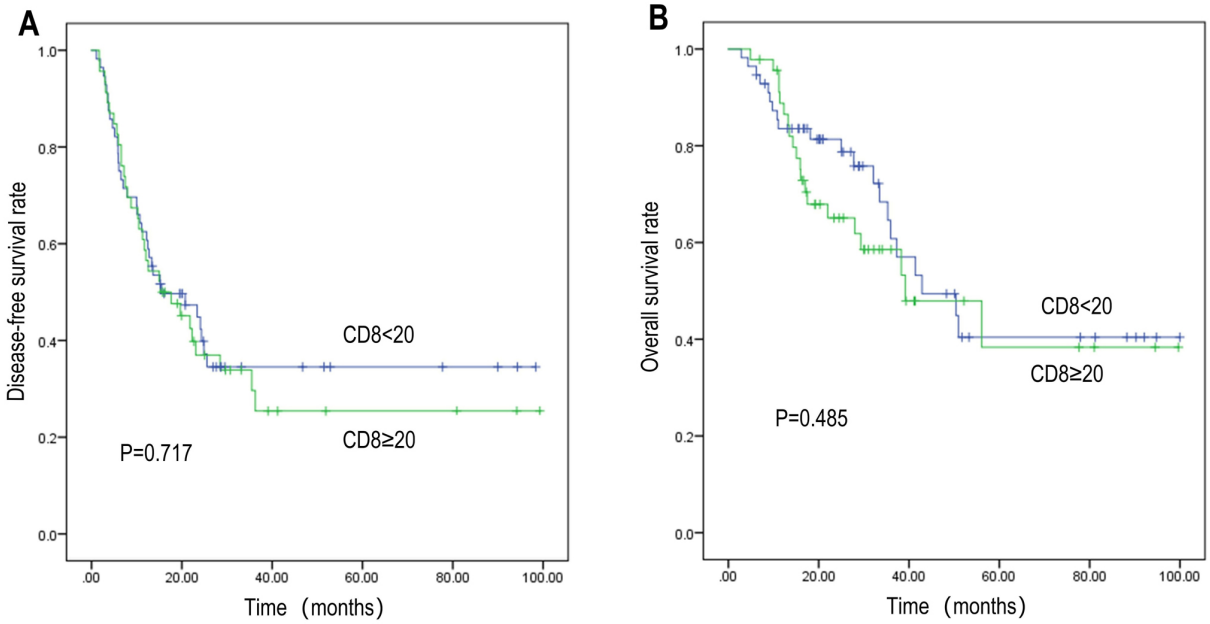

Figure S4. Kaplan-Meier curves showing CD45RO^{+} TILs were not significantly associated with (A) DFS or (B) OS in patients with ICC. DFS, disease free survival; OS, overall survival; ICC, intrahepatic cholangiocarcinoma; TILs, tumor-infiltrating cells.